

# Report on Shoreline Erosion in New Jersey After Hurricane Sandy

Author: Stafford Eamon Smith

Submitted: 5<sup>th</sup> June 2020

**Abstract:** *Hurricane Sandy caused dramatic change in the shoreline of the New Jersey coast. In this study Digital Surface Models (DSMs) of the New Jersey coast are created from publicly available LiDAR data acquired before and after the hurricane. These DSMs are used to assess height changes and determine areas of erosion and deposition in the beach zone. Lidar has been used in storm damage assessment to great effect, and a brief literature review and discussion of the strengths and limitations of the technique is included. The findings show that some dune destruction has certainly occurred on the New Jersey coast as a result of the storm, but further study is required to investigate this pattern more widely.*

# CONTENTS

---

List of Figures .....	3
1 Introduction .....	4
1.1 The Problem .....	4
1.2 Background .....	5
1.2.1 Background to the Storm Event .....	5
1.2.2 The Study Area .....	6
1.2.3 LiDAR and Shoreline Erosion Research .....	6
1.3 Aim and Objectives .....	8
1.4 Datasets and Equipment .....	9
1.4.1 EAARL-B Coastal Topography--Eastern New Jersey, Hurricane Sandy, 2012: First Surface, Pre-Sandy .....	9
1.4.2 2012 USGS EAARL-B Coastal Topography: Post-Sandy, First Surface (NJ) .....	9
1.4.3 Sentinel Imagery, pre and post Sandy. ....	9
1.4.4 Equipment .....	9
2 Method .....	10
2.1 Creation of Digital Surface Models .....	10
2.2 Deriving Elevation Change .....	10
2.3 Defining the Beach Area .....	11
2.3.1 Background .....	11
2.3.2 Unsupervised Classification .....	11
2.3.3 Filtering of Unsupervised Classification Results .....	12
2.4 Along-Shore Change Profile .....	13
2.5 Cross-Shore Change Profiles .....	14
3 Results .....	16
3.1 Erosion and deposition patterns – extreme cases .....	16
3.2 Erosion and deposition patterns – the beach .....	18
3.3 Along -shore profile .....	21
3.4 Cross-Shore Profiles .....	22
4 Discussion and Recommendations .....	24
4.1 Significance .....	24
4.2 Limitations .....	25
5 Conclusion .....	26
6 References .....	27
7 Appendix A .....	31

7.1	R code for creation of DSMs from raw lidar data .....	31
7.2	R code for creation of Damage raster.....	32
7.3	R code for unsupervised imagery classification and modal filtering .....	32
Appendix B	.....	35
1:20,000 map series of Morphological Change	.....	35

## LIST OF FIGURES

---

Figure 1. Hurricane Sandy Path – redrawn from (Blake et al., 2013, p. 127) .....	5
Figure 2. Study area along the New Jersey Coast.....	6
Figure 3. Sentinel 2A bands used in analysis. ....	11
Figure 4. Raw classification > Modal filter applied > Vectorised with GRASS smoothing algorithm. Beach is shown in white (raster classification cells) and yellow (final ‘Beach Area’ polygon). ....	12
Figure 5. Sampling strategy.....	13
Figure 6. Map showing location of cross-shore profile transects.....	15
Figure 7. Statistics for the height change dataset clipped to beach extent. ....	16
Figure 8. Extreme height decreases related to building destruction.....	16
Figure 9. Extreme height increases related to deposition of building debris.....	17
Figure 10. Classes used for display .....	18
Figure 11. Determination of class break values showing mean and standard deviations as dotted lines. ....	18
Figure 12. Overview of map tiles presented in Appendix A. ....	19
Figure 13. Excerpt from “Erosion and Deposition – Map J” .....	20
Figure 14. Excerpt from “Erosion and Deposition – Map M” .....	20
Figure 15. Along Shore Profile showing height change for sampling points .....	21
Figure 16. Transect 1, Deal Borough.....	22
Figure 17. Transect 2, Deal Borough.....	22
Figure 18. Transect 3, Deal Borough.....	23

# 1 INTRODUCTION

---

## 1.1 THE PROBLEM

Shorelines do more than provide a place a recreation – they are a critical morphological barrier to flooding of infrastructure, assist in the maintenance of freshwater tables against saltwater intrusion (Saye et al., 2005, p. 128), frequently have cultural heritage values, and are important ecological habitats in their own right. Perhaps the most critical component of this list in the near future will be the role of shorelines as barriers to flooding of settled areas. Worldwide, coastal zones host between 15% and 40% of the human population (Roebeling et al., 2018, p. 175). Dune systems are adaptable mobile barriers that protect settled areas from storm surge, but extreme events can overwhelm the capacity of the shoreline to provide this barrier (Saye et al., 2005).

Within the coming decades, shorelines are likely to face pressures from sea level rise and climate change (Burvingt et al., 2017, p. 722). While it is likely that the mobile nature of dune systems (Jackson et al., 2005) will be able to respond to the gradual sea level rise process in the short term, an increase in extreme weather events such as hurricanes that is thought to be concomitant with climate change (Emanuel, 2013) will put more immediate pressures on shoreline morphology (Burvingt et al., 2017; Fletcher et al., 2016). Extreme weather events such as hurricanes can overwhelm the system's capacity to respond, and the shoreline can be heavily eroded, reducing its capacity to act as an important barrier to flooding of settled areas. At the same time, increasing human population pressure is likely to increase the density of these vulnerable built up areas close to the shoreline (Fletcher et al., 2016, p. 1023). With this in mind, it is important that we characterise the effect of extreme weather events such as hurricanes on the morphology of shorelines, with particular mind to understanding how they might reduce the shorelines capacity to act as a morphological barrier to flooding and inundation of built up areas landward of the shoreline zone.

Shoreline erosion and attempts at mitigation pose a significant cost to managing bodies. For example, for the 1990 – 2020 period, public expenditure on coastline protection in the EU was estimated to exceed 5 billion Euros (Sellick, 2006). In England and Wales, approximately GBP 50 million is spent annually to mitigate coastal erosion (Penning-Rowsell & Pardoe, 2015).

## 1.2 BACKGROUND

### 1.2.1 Background to the Storm Event

The U.S. East coast is regularly under threat from tropical and ex-tropical cyclones and hurricanes (Liu et al., 2020). Shoreline erosion, coupled with storm surge, creates a very real threat of coastal inundation, consequential property and infrastructure damage, and indeed risk to human life. In this report I will analyse the effect of Hurricane Sandy (Figure 1) that made landfall on the New Jersey coast in October of 2012 (Sullivan & Uccellini, 2013). This storm resulted in enormous impacts to life and property in both the Caribbean and the continental United States, and the effects extended as far west as Wisconsin (Sullivan & Uccellini, 2013, p. iv), but the analysis in this report will be confined to the New Jersey coast, as described in section 1.2.2.

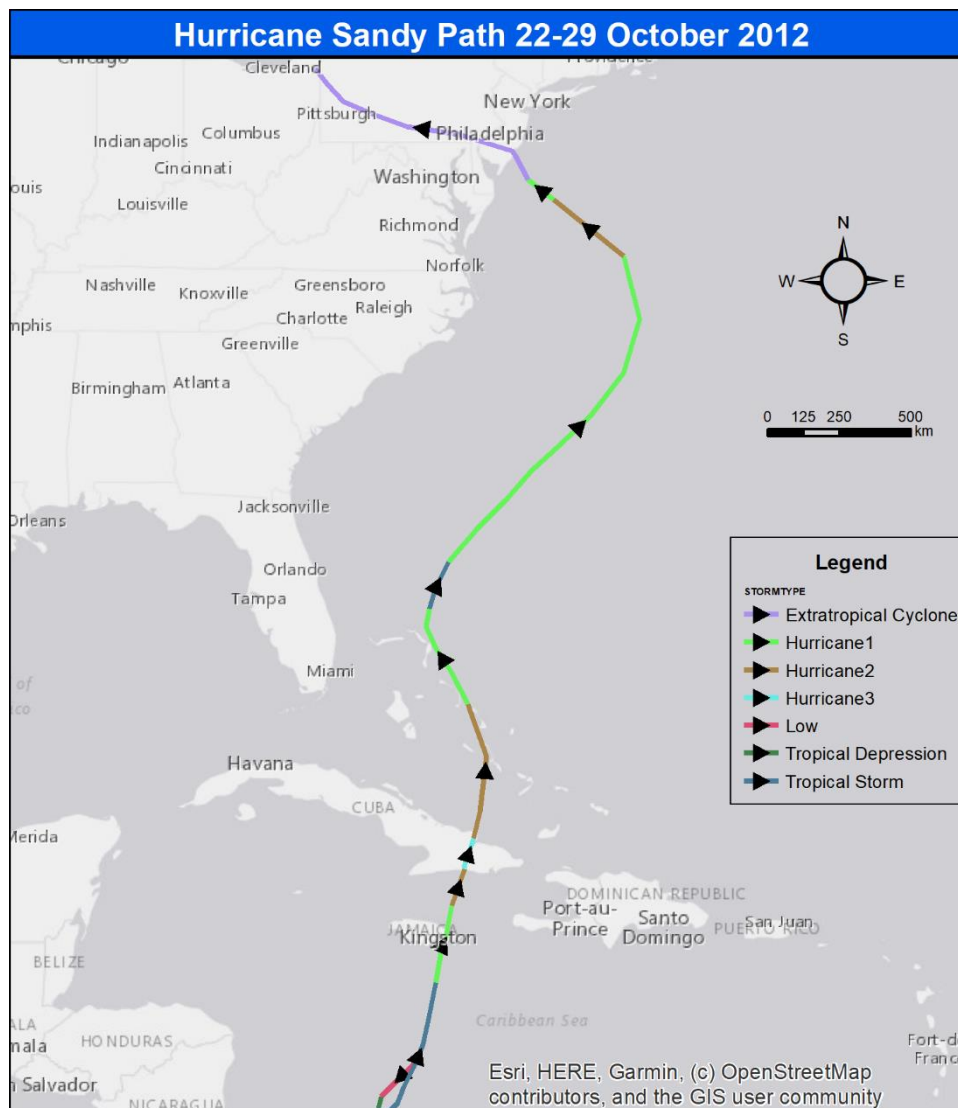


Figure 1. Hurricane Sandy Path – redrawn from (Blake et al., 2013, p. 127)

## 1.2.2 The Study Area

The study area is described in Figure 2. Please note that the actual analysis was only conducted at the beach zone as defined by beach sand, and further limited by those areas of the beach zone covered by our LiDAR dataset (shown in more detail, Figure 12).

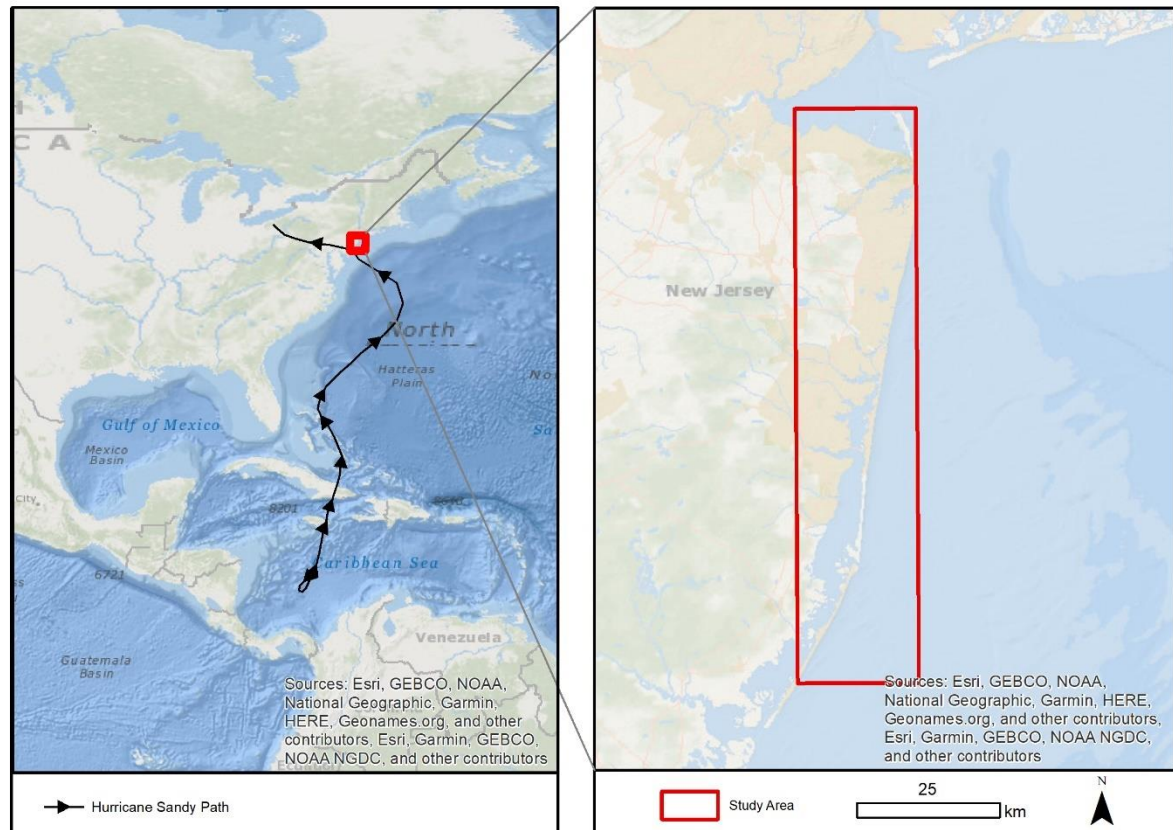


Figure 2. Study area along the New Jersey Coast.

## 1.2.3 LiDAR and Shoreline Erosion Research

Compared to other remote sensing techniques, the high level of spatial detail makes LiDAR an excellent tool to analyse changes in elevation profiles, and thereby to assess shoreline erosion. Especially, LiDAR datasets are characterised by highly accurate elevation measurements in comparison to other remote sensing techniques, which is of direct and obvious relevance to elevation analyses. LiDAR has been used extensively in morphological studies of coastal areas, and I will present a selection of key studies here.

Farris et al. discuss the US Geological Survey's response to the hurricanes of 2005 that included Katrina (Farris et al., 2007). They present diverse cases using remote sensing, and those using LiDAR discuss its advantages compared to other techniques. The Gesch article in this publication discusses using LiDAR to quickly estimate inundation in the days immediately after Hurricane Katrina (Gesch, 2007, pp. 53–55). Flood inundation depth was calculated using a LiDAR derived elevation profile combined with water level data. Gesch emphasises the superiority of LiDAR over other remote sensing methods for data acquisition where vertical accuracy and high spatial resolution is required (Gesch, 2007, p.

56). As a shoreline is defined by its elevation relative to tide height (Yang, 2008, p. 300), any assessment of shoreline erosion requires high vertical accuracy and high spatial resolution.

The article by Sallenger et al. in the same volume emphasises that the primary advantages of LiDAR over ground surveys are the speed of acquisition and high spatial density (Sallenger et al., 2007, p. 114). In the context of a time-critical response to an environmental disaster, LiDAR is an excellent tool precisely for its speed of acquisition. No other method with high spatial density and vertical accuracy can compete, with perhaps the exception of photogrammetry.

Photogrammetry provides one viable alternative to capture the kind of datasets needed to assess storm damage. Bevan et al. describe the trade-off between these two methods, with LiDAR being prohibitively expensive to acquire, and stereo-photogrammetry having limited spatial coverage OR resolution (George Bevan et al., 2012). Since the time of publication however, the availability of UAV based LiDAR has largely negated the expense of acquisition (e.g. Lee & Park, 2019).

Pye and Blott use LiDAR to analyse which parts of a dune system experienced the most erosion, finding that this occurred where the upper beach was less than 25m wide (Pye & Blott, 2016). This study is relevant to this report in that it emphasises that erosion occurs at different rates across a study area. Differential erosion is evident in the study area analysed in this report, and it is hoped that by using cross-shoreline elevation profiles these patterns can be investigated.

Cross-shoreline elevation profiles have been employed by Masselink et al. to analyse differential erosion in the dune, back-shore, and intertidal zones (Masselink et al., 2016). They employed 224 individual cross-shore transects from 38 beaches. Saye et al. also used cross-shore profiles to investigate zonal differences in erosion and deposition (Saye et al., 2005). Houser et al. use both along-shore profiles, and cross-shore profiles to demonstrate morphological changes (Houser et al., 2015).

Elevation change can be calculated using image differencing between a pre and post storm LiDAR dataset. Andrews et al. present their method to achieve this and found that, in their study, the greatest elevation reduction, and therefore erosion occurred along the seaward faces of dunes (Andrews et al., 2002).

Other studies take the analysis a step further and calculate sediment volume change pre and post storm, using LiDAR image differencing. Burvingt et al. conducted a sophisticated analysis, where they considered sediment volumetric change at different levels along the beach and found that beaches were either flattening (with upper beach erosion and lower beach accretion) or steepening (upper beach accretion and lower beach erosion) (Burvingt et al., 2017, pp. 731–732). Other volumetric change studies of shoreline morphology using LiDAR include Woolard and Colby (2002) and Houser et al. (2015).

Stoker et al used LiDAR to model the inundation of a landscape due to storm surge (Stoker et al., 2009). Richter et al. (2013) present a fascinating technique that uses moving Laplace and Sobel filters to detect abrupt height changes in their lidar data, and thereby identify the movement of dune cliffs over time. Whilst outside of the scope of this report, these two studies demonstrate that the high spatial resolution and vertical accuracy of LiDAR have opened up new avenues of research into shoreline morphological change.

### 1.3 AIM AND OBJECTIVES

The aim of this research is to determine the extent and character of shoreline change along the New Jersey coast due to Hurricane Sandy. In order to achieve this aim I will use LiDAR datasets acquired before and after the storm to derive digital elevation models (DEMs). From these DEMs I will model the elevation change along the shoreline. Whilst the available LiDAR data extends beyond the shoreline zone, I will restrict the analysis to the area defined by beach sand, using multispectral classification of (non-contemporaneous) Sentinel imagery to derive a study area extent. To examine the character of the shoreline change in detail, I will investigate the shoreline in the Borough of Deal with cross-shoreline elevation change profiles.

## 1.4 DATASETS AND EQUIPMENT

The following datasets have been used in this report.

### 1.4.1 EAARL-B Coastal Topography--Eastern New Jersey, Hurricane Sandy, 2012: First Surface, Pre-Sandy

Inspection of the metadata does not clearly indicate the date the original data was acquired. This is not ideal, but does not preclude analysis as it is emphasised that the data is 'Pre-Sandy'. The data has been provided by the National Oceanic and Atmospheric Administration Office for Coastal Management. Data is in EPSG:5703 coordinate reference system.

The data is in the form of an xyz point cloud, and the extent is of a portion of the New Jersey coastline, pre-Hurricane Sandy. The data was acquired with aircraft based LiDAR called the Experimental Advanced Airborne Research Lidar (EAARL-B). Average points spacing is 0.5-1.6m.

This dataset consists of 10x10km extent tiles. Importantly, the metadata reveals that the entire dataset was captured in the same flight, was processed together and only subsequently split into tiles, so I do boundary issues between the tiles should be minimal.

The dataset is accessible at [https://coast.noaa.gov/htdata/lidar1\\_z/geoid12a/data/3658/](https://coast.noaa.gov/htdata/lidar1_z/geoid12a/data/3658/)

### 1.4.2 2012 USGS EAARL-B Coastal Topography: Post-Sandy, First Surface (NJ)

The post-sandy dataset has been derived using the same sensor and processing method as the pre-sandy dataset. This is ideal for our analysis.

### 1.4.3 Sentinel Imagery, pre and post Sandy.

Sentinel Imagery will be used to restrict our analysis to the beach areas of the study area. A unsupervised classification method will be used to spectrally classify the Sentinel images and derive an extent shape for the beach area (see Section 2.3.2).

Sentinel imagery is not available contemporaneous with the study period. I have chosen recent imagery that covers the study area, and has <5% cloud cover.

Two adjacent and contemporaneous Sentinel 2 scenes were chosen:

S2A\_MSIL2A\_20200308T154101\_N0214\_R011\_T18TWK\_20200308T200723

S2A\_MSIL2A\_20200308T154101\_N0214\_R011\_T18SWJ\_20200308T200723

They were both acquired on the 8<sup>th</sup> of March 2020, with the same sensor.

### 1.4.4 Equipment

All data processing, analysis, and visualisation was carried out on a Microsoft Surface Book 2, with an Intel i7 processor and 16gb of RAM, running a Windows 10 operating system. Software used includes:

- R (and R-Studio as GUI)
- QGIS 3.12.2
- GRASS GIS 7
- ArcMap 10.5, Spatial Analyst extension

## 2 METHOD

---

### 2.1 CREATION OF DIGITAL SURFACE MODELS

The aim for this step was to take the raw LiDAR data, consisting of .las tiles and metadata, and to create digital surface models of the study area in its pre-hurricane and post-hurricane state. LiDAR processing was performed in R (R Core Team, 2013).

The 'grid\_canopy' tool from the 'lidR' R package was used to create Digital Surface Models from the raw LiDAR data. This allows a choice of algorithms, and the 'dsmtin' Digital Surface Model Algorithm was used (see <https://rdr.io/cran/lidR/man/dsmtin.html>). Output resolution was set to 2m to provide a balance between high resolution and ease of data processing and speed.

A critical decision was made at this point in the method. Unique amongst remote sensing methods, LiDAR data has multiple returns, which allows users to map the surface of the terrain (a Digital Terrain Model) or objects above this surface, commonly vegetation and buildings (a Digital Surface Model). As part of the intention of this report is to study the damage to all parts of the shoreline, it was decided to examine the change in the first return values, or between Digital Surface Models. For a strict analysis of dune morphology, different results may be obtained by deriving Digital Terrain Models and performing difference analysis on these (please see Section 4.2 for a discussion of this point).

Two Digital Surface Models were created:

DSM\_PRE\_FULL.tif, a 2x2m raster dataset, with cell values representing local height pre-hurricane.

DSM\_POST\_FULL.tif, a 2x2m raster dataset, with cell values representing local height post-hurricane.

Please see Section 7.1 of this report for the R code used to derive the Digital Surface Models.

### 2.2 DERIVING ELEVATION CHANGE

This step was also performed in R (R Core Team, 2013). The Digital Surface Models created in Section 2.1 consist of rasters with height values specified in meters. The elevation change raster was derived using a basic mathematical operation in R, whereby the height of each cell in the PRE DSM was subtracted from the height of each cell in the POST DSM. The resulting raster shows the height difference due to the storm for each 2x2m cell.

Please see Section 7.2 of this report for the code.

## 2.3 DEFINING THE BEACH AREA

### 2.3.1 Background

The study area was restricted to the beach zone for two reasons. Firstly, by restricting the study to this area, we could focus our analysis on deposition and erosion of this zone, without being distracted by changes in other areas. Specifically, the range of height change values in our dataset would be specific to our question, and would allow our visualisations to reflect the changes that we are interested in in greatest detail, without being distracted by more extreme changes in other parts of the image, such as building destruction in the built environment landward of the dunes.

Secondly, the study area was restricted to the beach zone as these processes are computationally and memory intensive. It could be said in the past that the large size of LiDAR datasets was a disadvantage, but with the constant development and availability of processing power this is becoming less of an issue.

### 2.3.2 Unsupervised Classification

A recent Sentinel 2 scene was downloaded from the Copernicus Open Access Hub (<https://scihub.copernicus.eu/dhus/#/home>), with the intention to perform land cover classification to identify the beach zone. The image chosen was a recent image, as no affordable 10m resolution imagery was available at the time of the hurricane, and the actual beach area has not changed significantly since that time. The imagery was processed in the SNAP software (*SNAP - ESA Sentinel Application*, 2019) using the 'S2 Resampling Processor' tool. This allowed me to create 10m resolution version of the 20m bands (Figure 3). Please note, the chosen scene was acquired using the 2A sensor and the spectral information in the table is specific to that sensor.

Band	Description	Central wavelength (nm)	Bandwidth (nm)	Resampling
2	Blue	492.4	66	-
3	Green	559.8	36	-
4	Red	664.6	31	-
5	RE1	704.1	15	20m > 10m
6	RE2	740.5	15	20m > 10m
7	RE3	782.8	20	20m > 10m
8	NIR	832.8	106	-
8A	NNIR	864.7	21	20m > 10m
11	SWIR1	1613.7	91	20m > 10m
12	SWIR2	2202.4	175	20m > 10m

Figure 3. Sentinel 2A bands used in analysis.

In the course of my research I identified a process called super-resolving, whereby the 20m bands could be resampled to 10m by a complex series of algorithms that would actually result in a dataset with additional information that could be used for multispectral classification. In some cases this may be useful, but given that we only want to identify beach areas which have a very distinct spectral signature, the process (which is very computationally intensive) was deemed unnecessary.

The resulting 10m dataset of 10 bands was processed in R and unsupervised classification performed. Unsupervised classification with two classes separated water and everything else. Unsupervised classification with 3 classes separated sand, water, and everything else. Visual inspection in ArcMap revealed that the classification of the sand areas resulting from a 3-class unsupervised classification was accurate enough for our purposes, and supervised classification was deemed unnecessary. Please see Section 7.3 of this report for the R code used for this step.

The unsupervised classification was performed using the tool 'unsuperClass' from the R toolbox 'RStoolbox'. This tool implements a K-Means algorithm described by Hartigan and Wong (1979).

### 2.3.3 Filtering of Unsupervised Classification Results

Modal filtering reduced the complexity of the classification and resulted in a more continuous beach extent. Figure 4 shows an example of the result of this process, which will suit the purposes of the analysis.



Figure 4. Raw classification > Modal filter applied > Vectorised with GRASS smoothing algorithm. Beach is shown in white (raster classification cells) and yellow (final 'Beach Area' polygon).

To neaten the data, further processing was performed. The beach is mostly a continuous area in reality, and the classification picked up some white building roofs and other small areas with a similar spectra signature that it would be useful to exclude. To achieve this, the raster was converted to polygons using the GRASS algorithm 'r.to.vect', with smoothing enabled. This was run inside an instance of QGIS, in preference to the native QGIS algorithms, as it is more efficient in handling large datasets. Small outlying polygons were filtered out manually by visual map inspection and deletion, assisted by area calculation for each polygon feature. The result of this process was a polygon shapefile, which will be referred to as the 'Beach Area' henceforth.

The damage raster was cropped to the 'Beach Area' extent using the GDAL tool 'Clip raster by mask layer' running inside an instance of QGIS.

## 2.4 ALONG-SHORE CHANGE PROFILE

To examine height change along the entire coastline of the study area, a sampling strategy was employed to place a point roughly every kilometre along the beach. As our beach is a complex shape, it was not possible to draw a straight transect along its entire length. However, the study area is roughly north-south oriented, and this assisted in the design of a replicable sampling strategy. Points were spaced by 1000m in their UTM Northing value, and were assigned to the horizontal centre of the beach polygon at that northing. This is demonstrated in Figure 5.



Figure 5. Sampling strategy

Sampling points were generated in QGIS version 3.12.2 using the following process, developed to suit the unique requirements of the sampling strategy:

- 1) Created a 1000m x 1000m grid with the extent of the 'Beach Area' polygon (described in Section 2.3), using the tool *Vector > Research Tools > Create Grid*
- 2) Horizontal lines only were selected from the grid using the following Select by Expression:

```
y_min($geometry) = y_max($geometry)
```

- 3) These horizontal lines were clipped to be the width of the 'Beach Area' polygon at their location by performing an Intersection analysis using the tool *Vector>Geoprocessing Tools>Intersection*
- 4) The centre of each of these line segments was found using *Vector>Geometry Tools>Centroids*, thereby positioning the sampling point at the horizontal centre of the 'Beach Area' polygon for that UTM Northing value.

The sampling points were used to extract raster values at their location. This was accomplished using the GRASS GIS tool "v.what.rast" running within QGIS. Using this tool, I added the value of the

“Damage” raster created in section 2.2 to the attribute table of our sampling points. Next, I added the UTM Northing value for each point using the Field Calculator in QGIS. These attributes were then saved as a comma delimited text file and imported into Microsoft Excel. Excel was used to map the relationship between Northing and height-change. The results are presented in Section 3.3.

## 2.5 CROSS-SHORE CHANGE PROFILES

To further characterise the nature of the erosion patterns, I established three cross-shore transects in the Borough of Deal. These transects were used to create height change profiles to examine how erosion effect changed with distance from the shoreline. The Borough of Deal was chosen as it is anecdotally known to have been particularly hard hit by the Hurricane. The transects were purposefully positioned in a part of the coastline in Deal where a repeated pattern of heavy erosion close to the dunes was observed (please refer to Section 3.2 for further explanation of this phenomena).

The transects were digitised in ArcMap 10.5, positioned to be approximately perpendicular to the shoreline. They extend from one edge of the “Beach Area” to the opposite edge, using the snapping tool. The location of the transects in relation to the Borough of Deal is shown in Figure 6 on the next page.

These transects were used to obtain raster values for the PRE and POST Digital Surface Models using the following steps in QGIS:

- 1) QGIS>Vector geometry>Points along geometry  
Added points every 1m along each of the transects using this tool
- 2) Reprojected to points to EPSG: 3625 (the coordinate system of the DSM rasters)
- 3) Used the SAGA tool “Add raster values to points” running within QGIS to add the values of the Pre-Hurricane, Post-Hurricane, and Damage rasters to the points file.
- 4) Exported the attribute table to a delimited text file
- 5) Plotted the results in Excel

These results are described in Section 3.4.

# Deal Borough - Overview

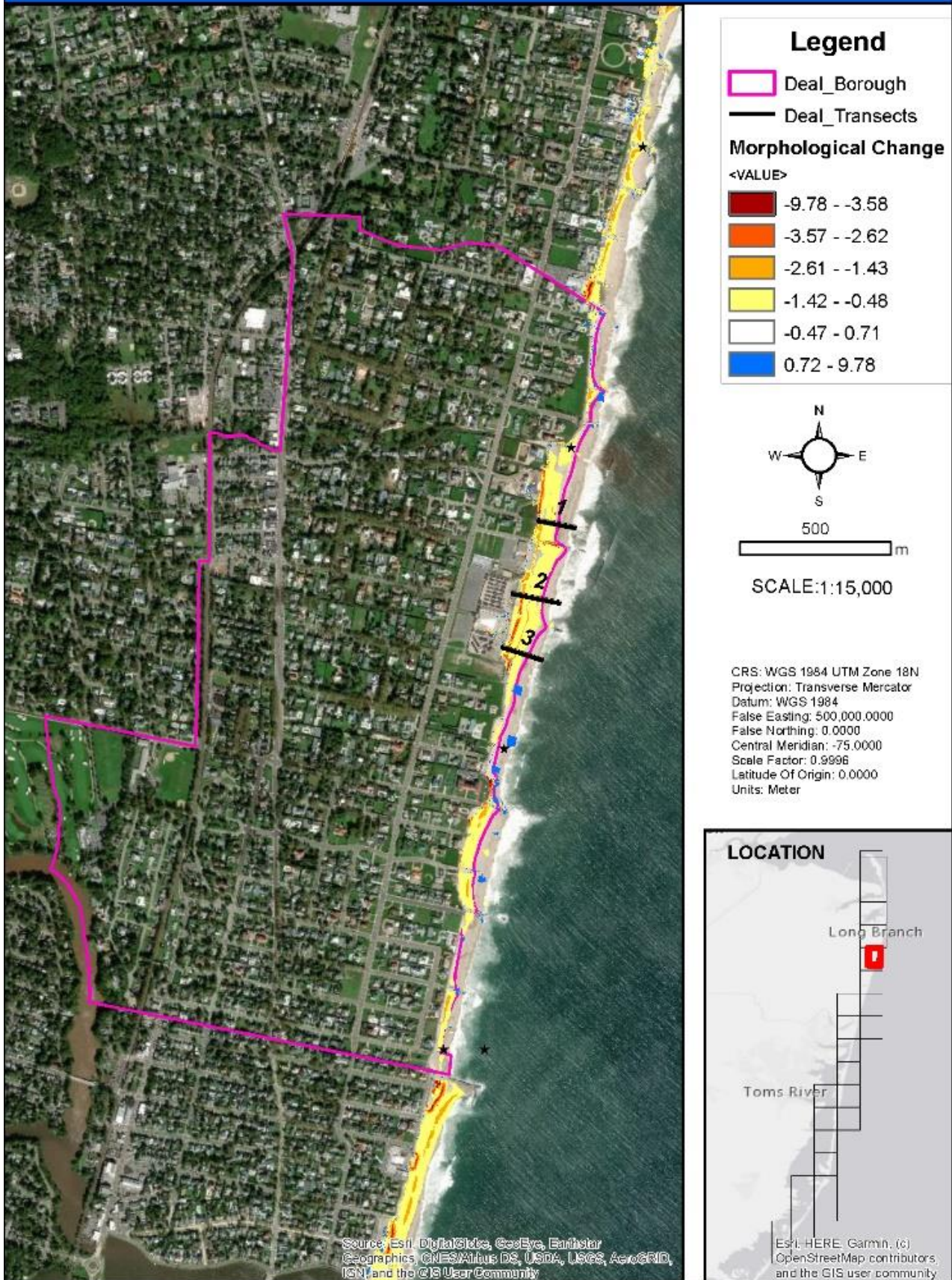


Figure 6. Map showing location of cross-shore profile transects

### 3 RESULTS

#### 3.1 EROSION AND DEPOSITION PATTERNS – EXTREME CASES

Erosion and deposition values were found to range from approximately -32m to 29m (see Figure 7). The values at the lower end of the spectrum most likely represent destruction of buildings. As the classification of the ‘beach extent’ study area used modern imagery, areas that are now sand once had buildings, and the extreme erosion values represent their destruction (see Figure 8). Whilst my first thought was to exclude these areas, they are an important result in their own regard, and one cannot in good conscience exclude these areas from the results.

<i>Min</i>	-32.20
<i>Max</i>	28.62
<i>Mean</i>	-0.80
<i>Std dev.</i>	1.07

Figure 7. Statistics for the height change dataset clipped to beach extent.

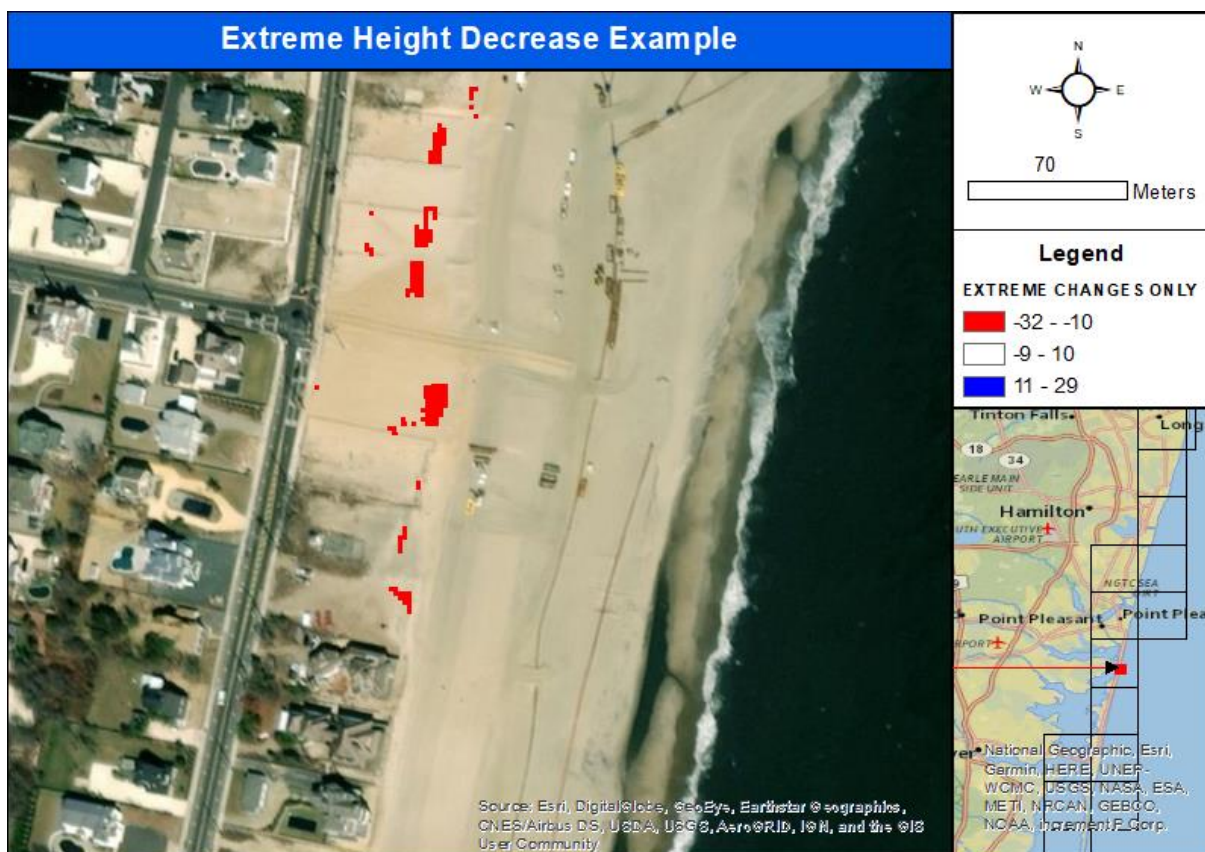


Figure 8. Extreme height decreases related to building destruction

The upper end of the change values, up around 29m, are possibly due to new buildings or the deposition of destroyed building material. The blue feature in Figure 9 shows a sudden height increase of between 12 and 20m, very close to a multiple areas of what appears to be building destruction. Each of the extreme height increase zones is similarly positioned, and I believe them to represent fallen buildings or destruction debris.

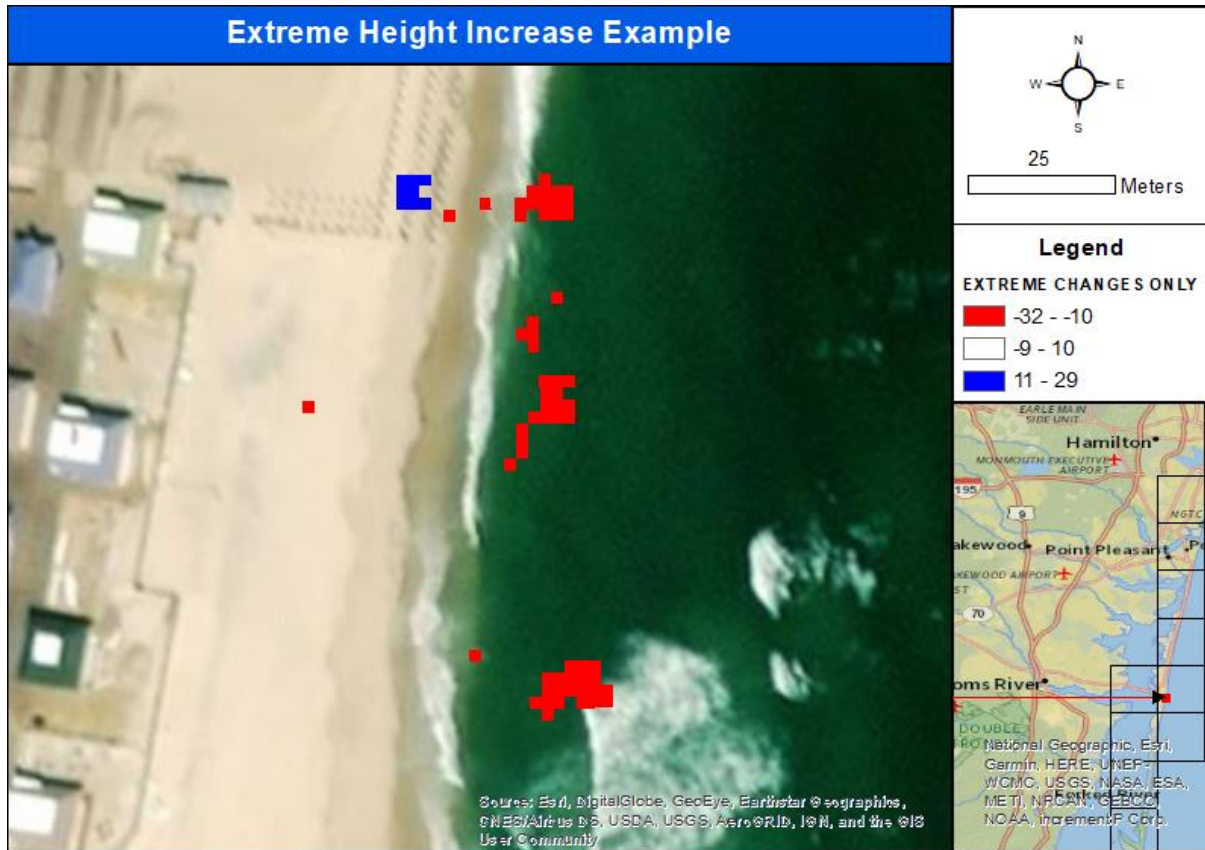


Figure 9. Extreme height increases related to deposition of building debris

### 3.2 EROSION AND DEPOSITION PATTERNS – THE BEACH

The remainder of the analysis is concerned with the change to the beach as a natural morphological feature, and extreme height change areas due to destruction of the built environment must be excluded for us to view these finer changes with sufficient detail. Extreme values with an elevation change greater than 10m were excluded on both sides of the value range, and erosion and deposition patterns and deposition was mapped using the following classes:

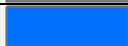
Colour	Lower Bound	Upper Bound
	-9.78	-3.58
	-3.57	-2.62
	-2.61	-1.43
	-1.42	-0.48
	-0.47	0.71
	0.72	9.78

Figure 10. Classes used for display

The classes (Figure 10) are based on standard deviations about the mean (see Figure 11), both of which have been recalculated after the removal of extreme values. Erosion is symbolised by a colour ramp from yellow to red. Area with little changed are not coloured. And areas of significant deposition are coloured blue. This symbology was arrived at by a heuristic process of trial and error, with reference to standard cartographic principles.

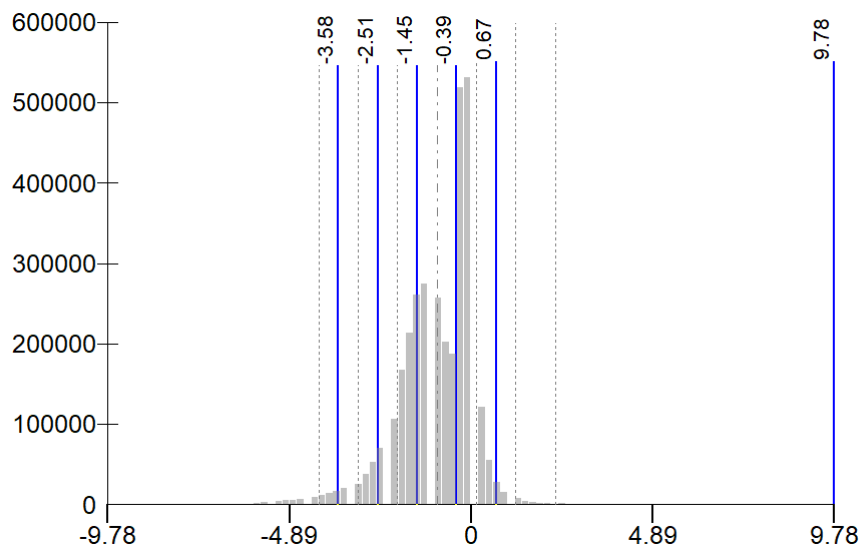


Figure 11. Determination of class break values showing mean and standard deviations as dotted lines.

Given that the study area is an elongated area roughly 100km long and 100m wide, the erosion and deposition patterns must be mapped in a series of maps to give a useful representation of what would otherwise be a very narrow feature. The extents of the tiles from the original LiDAR dataset provided a ready-made choice for the display extent of each map. A 1:20,000 map series is provided in Appendix B. All the maps in Appendix B are in WGS 1984 datum, UTM Zone 18N projection. An overview is provided here in Figure 12.

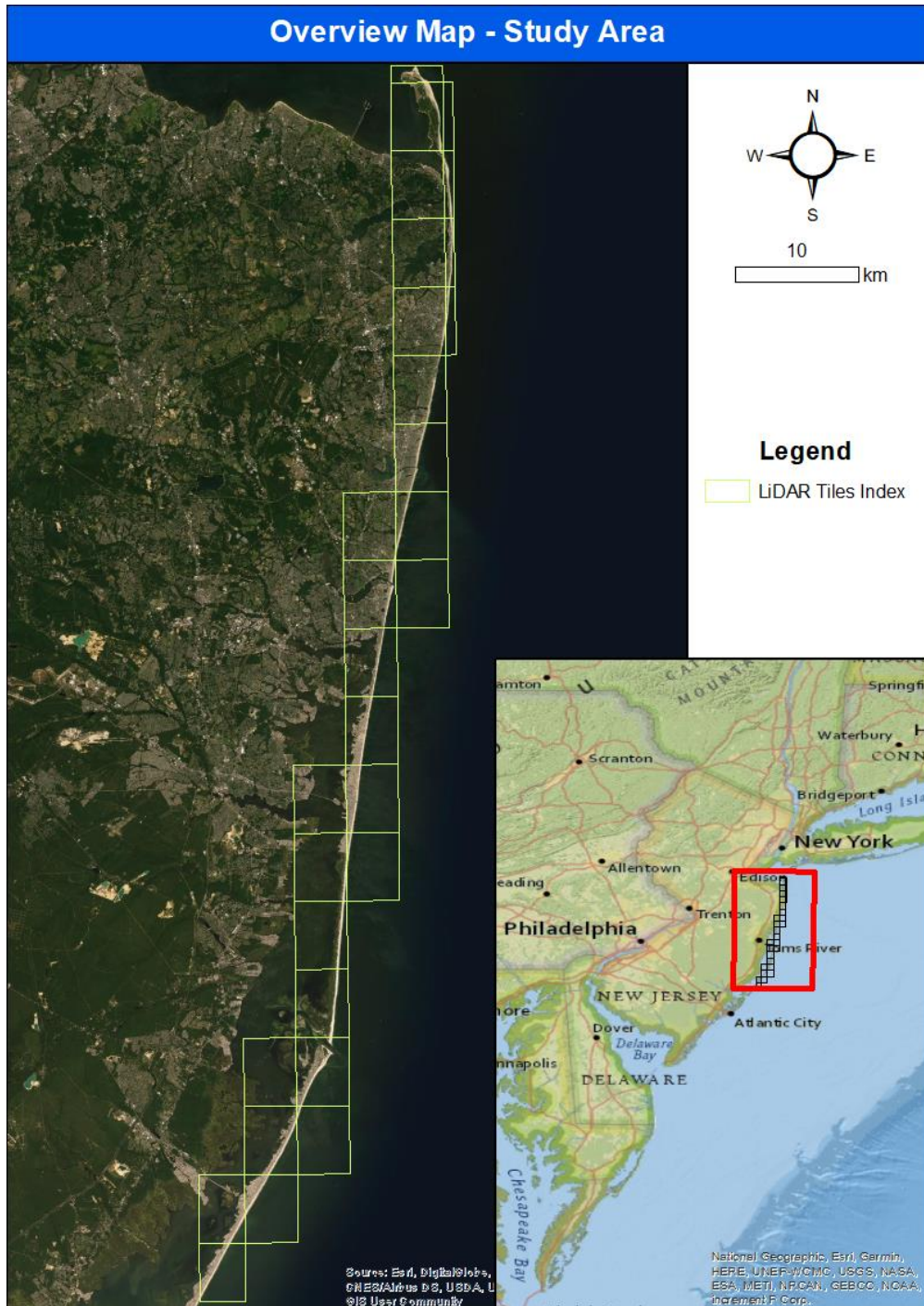


Figure 12. Overview of map tiles presented in Appendix A.

The Morphological Change map series (Appendix B) shows that erosion has taken place along the entire shoreline of the study area. These maps suggest that the erosion is not uniform, but that it is patterned.

Eleven of the nineteen morphological change maps reveal that the most heavily eroded areas lie towards the dune side of the beach. This is well illustrated in Figure 13 and Figure 14. The results of the cross-shore profile analysis supports and extends this pattern (described in Section 3.4).



*Figure 13. Excerpt from "Erosion and Deposition – Map J"*

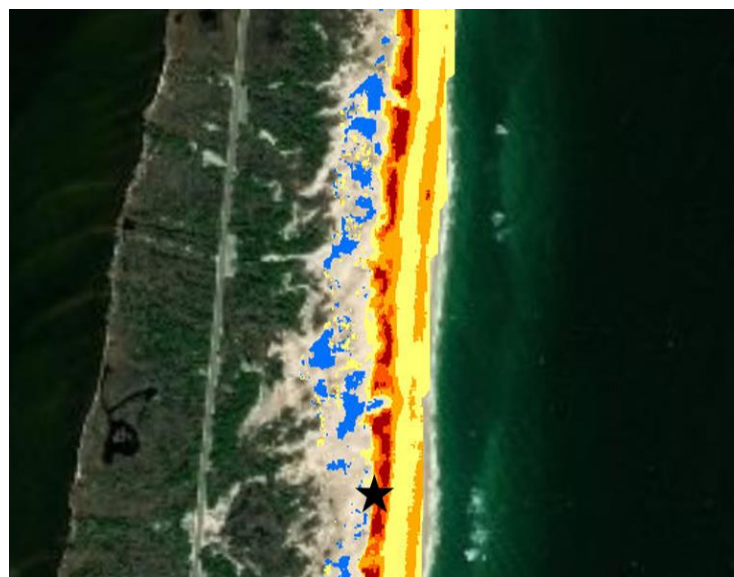


*Figure 14. Excerpt from "Erosion and Deposition – Map M"*

### 3.3 ALONG -SHORE PROFILE

The along-shore profile that resulted from the method outlined in Section 2.4 is given in Figure 15. A trend line has been calculated using a moving average of the nearest 10 values in an attempt to smooth the dataset in a meaningful way.

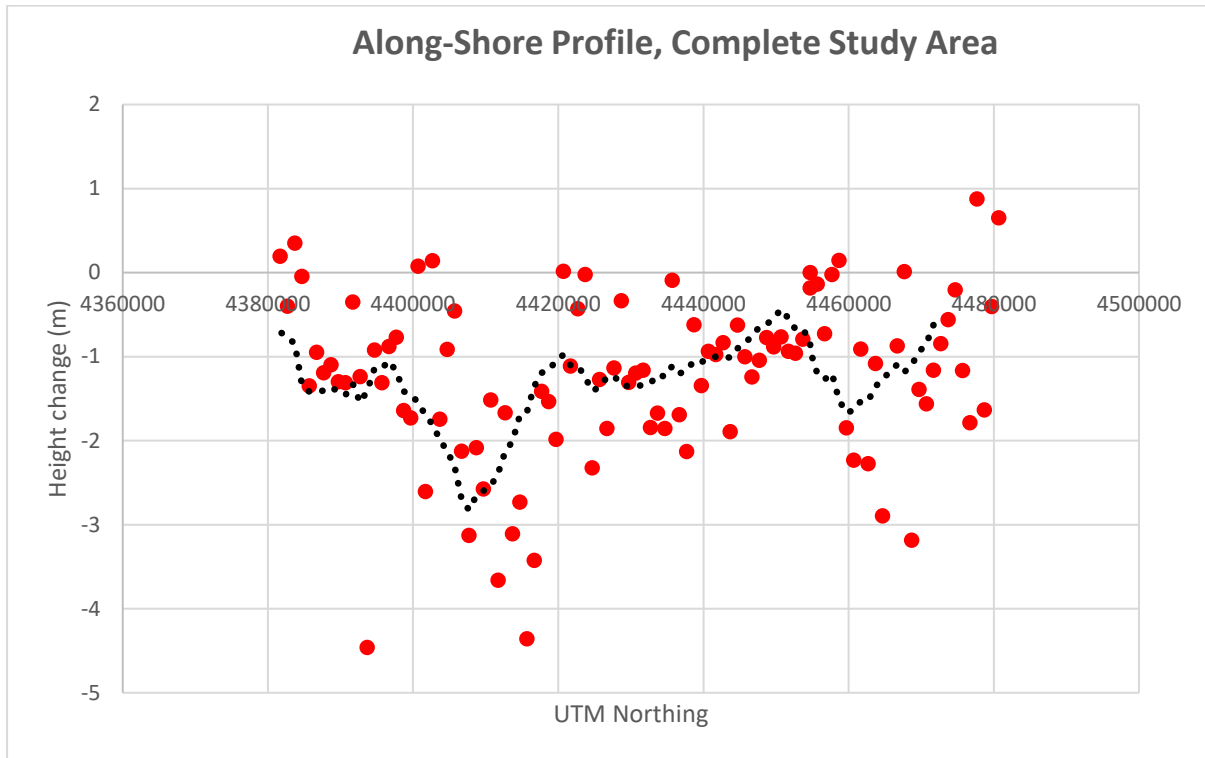


Figure 15. Along Shore Profile showing height change for sampling points

Of 100 sampling points, there was an average height reduction of 1.24m. 90% of the sampling points experienced height loss, and only 10% experienced an increase in height. This shows that erosion far outweighs deposition due to the storm. The coastline has been greatly eroded. Please see Section 4 for further discussion of these results.

### 3.4 CROSS-SHORE PROFILES

Cross shore profiles from the three transects in the Borough of Deal are presented in Figures 16-18.

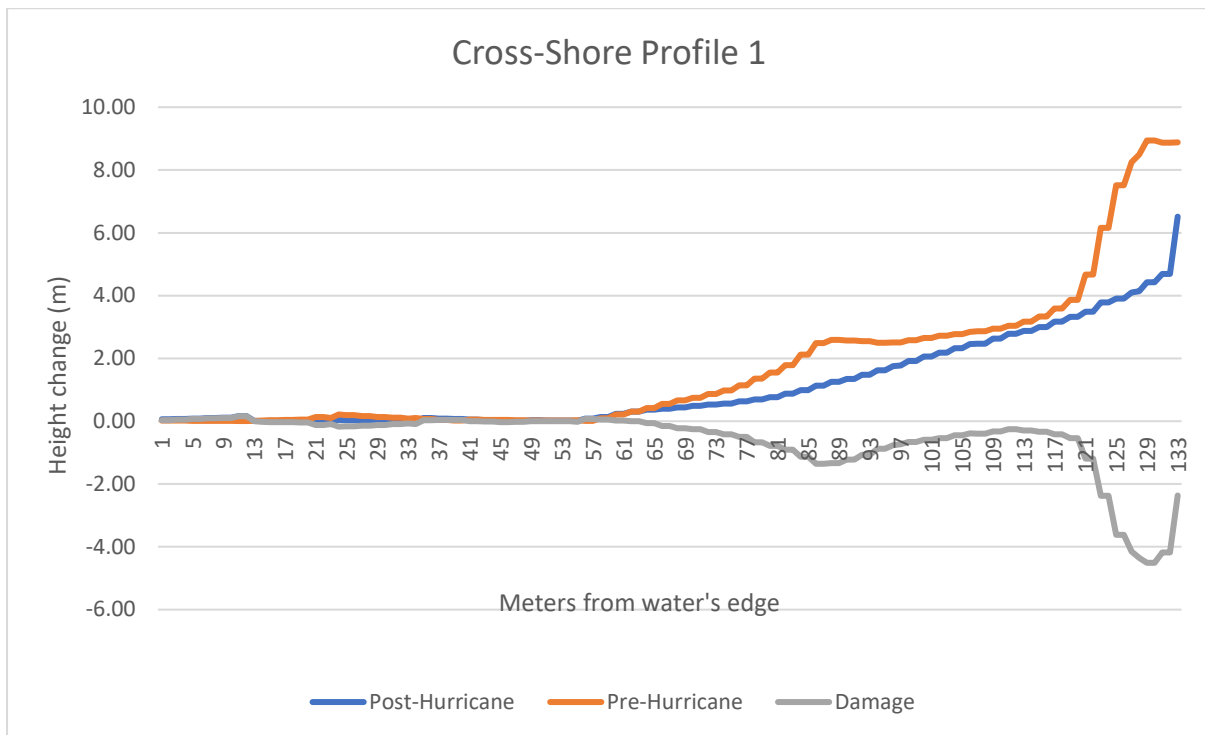


Figure 16. Transect 1, Deal Borough

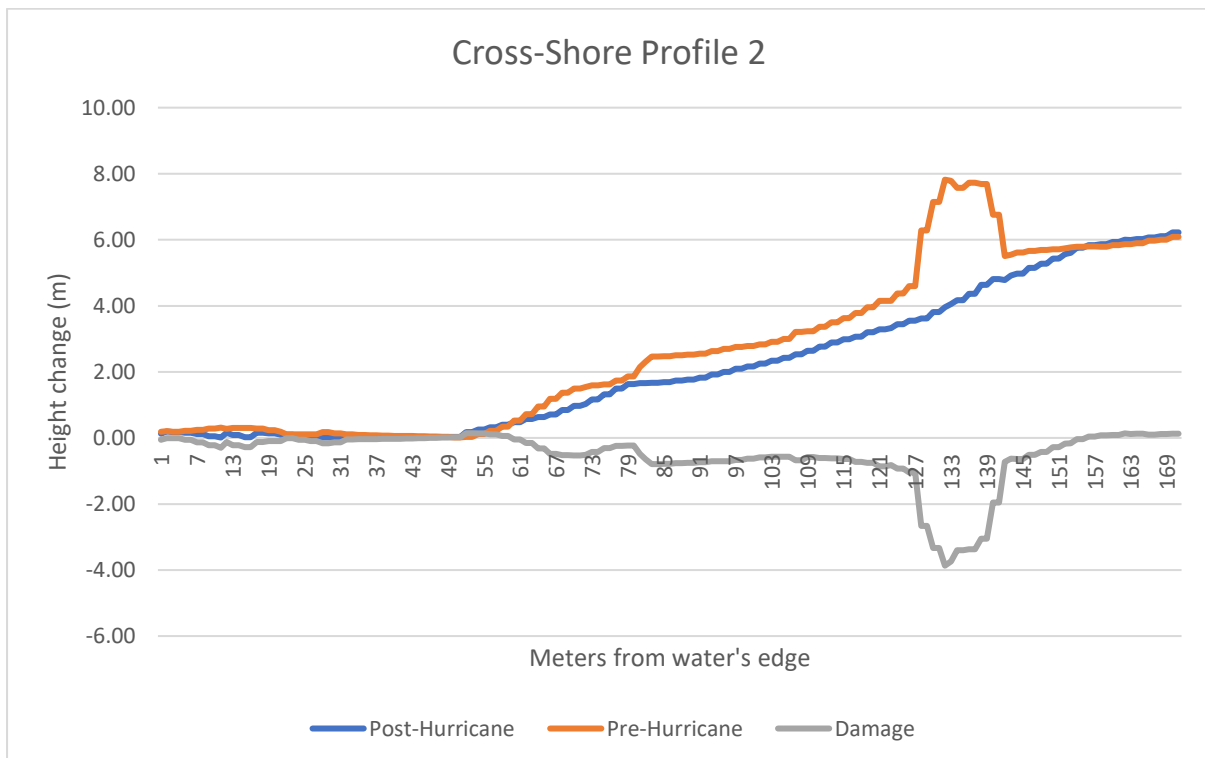


Figure 17. Transect 2, Deal Borough

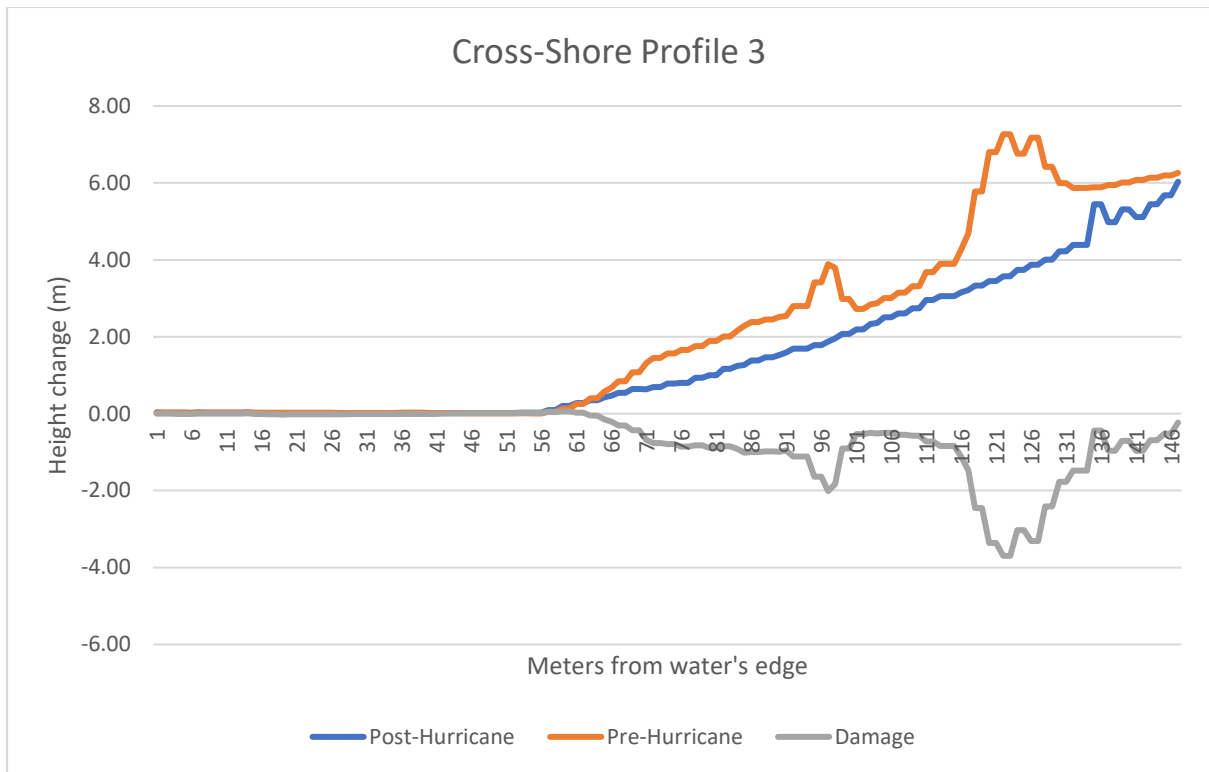


Figure 18. Transect 3, Deal Borough

The cross-shore profiles show that in all cases elevated features have experienced drastic levelling. The greatest height reduction has occurred in those parts of the cross-shore profile where a topographic elevation feature existed before the storm. This process has affected every raised feature in our transects, and hints at a significant and identifiable process at work that may be worthy of further study. Please see Section 4 for an interpretation of these results.

## 4 DISCUSSION AND RECOMMENDATIONS

---

### 4.1 SIGNIFICANCE

The results show that erosion has occurred along the entire shoreline of the study area. All maps in the 'Morphological Change' series (Appendix B) show erosion to some degree along the entire length of the beach. There is an average erosion of 1.24m from the sampling points, which is extreme in the context of the middle a beach zone where they were positioned. Whilst it can be said that extreme erosion has occurred, and far outweighs deposition, in this report I also aimed to characterise the nature of that erosion. Specifically, the context of this report is the premise that extreme weather events can change the morphology of a shoreline in a way that reduces its capacity to act as an important barrier to flooding of settled areas.

Figures 13 and 14 above are examples of the pattern present in eleven maps of the 19 Morphological Change maps: that erosion is greatest towards the dune side of the beach area. The cross-shore profiles were established to investigate this pattern – what do they reveal might be happening?

The cross-shore profiles (Figures 16-18 above) show that all features that present as a local topographic rise have been destroyed and levelled by the storm. These topographic features are almost certainly sand dunes. The implication is that this extreme weather event has levelled the sand dunes on the landward side of the shoreline. Cross-shore profiles were only established in the Borough of Deal, so it at this stage it is not possible to extrapolate this finding to the rest of the study area with any scientific reliability. However, this provides the impetus for the generation of a testable hypothesis for further research.

Two points are of relevance: firstly, the same general pattern of greatest erosion towards the landward side of the beach area is observable along most of the coastline as revealed by the Morphological Change maps; secondly, when that pattern was investigated in the Deal area it appears to represent the destruction of the barrier dunes. Given these two points, there are strong grounds to hypothesise that Hurricane Sandy has damaged the sand dunes along much of the coastline in a similar way. If this is the case, then the case may be made that this extreme weather event has impacted the coastline in a way that has reduced its capacity to act as a barrier to inundation of settled areas.

These findings echo those of Andrews et al. who found that the greatest storm erosion was occurring along the seaward face of dunes (2002). The findings, when examined in the light of the existing literature, show a clear path forward for further research. Pye and Blot examined which parts of a dune system experienced the most erosion, finding that this occurred where the upper beach was less than 25m wide (Pye & Blott, 2016) – does this relationship exist along the New Jersey shoreline? Certainly, erosion has occurred, and likely extensive barrier dune destruction has occurred. But is this phenomenon expressed to an equal degree along the entire length of the study area? As Burvingt et al. note, coastlines can exhibit a range of spatially variable and complex morphological responses, even though they have been subjected to the same extreme weather events (Burvingt et al., 2017, p. 722).

Further research is also required into the specific morphodynamics underlying the premise that dunes protect against inundation in this specific area. Fernández-Montblanc et al. discuss existing research in this direction (Fernández-Montblanc et al., 2020), but the focus has been on revegetation to stabilise dune systems: the morphodynamic role of dunes as a barrier to inundation has often been

taken as a given. Certainly, the height of a dune system relative to the storm surge must be the primary relationship in determining the potential of a dune-system to protect against inundation. At the very least, further research into recorded and predicted storm surge heights, and terrain modelling of the settled areas landward of the dunes should be undertaken before assumptions are made pertaining to the role of the New Jersey dune systems in flood mitigation.

## 4.2 LIMITATIONS

The method for determining the 'Beach Area' could be improved. The method used (Section 2.3) resulted in an extent that did not include all beach when visually inspected: it is likely that this is due to the different spectral signatures presented by wet and dry sand (e.g. Sekovski et al., 2014). Unsupervised classification is an expedient approach that was appropriate given the constraints of this research, but a more accurate study area could be determined by using high resolution imagery contemporaneous with the study period, coupled with a supervised classification process using human digitised training data. Indeed, the 'Beach Area' extent is the weakest part of the analysis, with even some areas missed from the beach classification due to cloud cover (e.g. Erosion and Deposition – Map D in Appendix A).

Burvingt et al. digitised every beach area manually by drawing polygons in ArcMap, and it is possible that this would provide the most accurate and precise result (Burvingt et al., 2017, p. 725). Even in this case, the beach areas they defined are not perfect, as by their nature shorelines are dynamic phenomena.

The along-shore profile (Figure 15) shows that erosion has been more extreme than deposition, but aside from this general statement, no other clear relationship exists between northing value and height change. Whilst there may be a relationship in reality, the sampling strategy employed in this study (described in Section 2.4) does not account for the complex nature of the shoreline change. At any one east-west transect through the beach zone, there are areas of deposition, erosion, and areas of no significant change: a sampling point in the center of this transect could lie in any one of these three situations. To characterise trends more accurately along the beach, a sampling strategy that averages the height change at that east-west location would be more appropriate. One approach would be to sum the area under a cross shore profile change curve every 1000m. These areas could be normalised by beach width. This approach could be carried out programmatically.

It is important to note that this study has been performed using Digital Surface Models – derived from the first return measured by the LiDAR instrument. It is possible that Digital Terrain Models derived from the secondary returns captured by the LiDAR instrument would provide a more appropriate dataset for any further study where the intention was to focus solely on the morphological changes undergone by the beach sand.

## 5 CONCLUSION

---

Shorelines provide an important barrier to flooding of settled areas. This report has demonstrated that extreme weather events have the potential to reduce the capacity of shorelines to provide this barrier. Whilst we have demonstrated that this capacity has been reduced due to dune damage in the Deal area, we have not quantified the extent of this change for the study area as a whole. This study serves to highlight an important pattern that deserves more rigorous assessment – that the hurricane has actually destroyed dunes. Further work is required to assess and quantify this pattern.

The findings in this report indicate that cross-shore profiles are a very powerful tool to assess the nature of shoreline erosion. Unless a suitable sampling strategy is employed, they are arguable more powerful than along-shore profiles. Further study could be directed to along shore profiles, but a more efficient approach is to work to understand the nature of the erosive patterns as they relate to the morphology of a shoreline at any one cross-shore transect. The relationships between erosion and shoreline morphological zones elucidated by this approach then have potential to be applied to any area. I feel that the cluster analysis approach of Burvingt et al. to investigate the relationship between erosion and morphological zones (2017) shows the greatest promise to further develop our understanding of the nature of storm induced shoreline damage.

With the likelihood of increased extreme weather events in the coming years, it is critical that funding be directed towards increasing our understanding of the character of shoreline damage. This will directly inform shoreline damage mitigation strategies. In the coming decades, without the barrier that shorelines provide to storms and inundation, a large segment of the world human population will be put at risk, and a more compelling reason for research does not exist than to mitigate this suffering.

## 6 REFERENCES

---

- Andrews, B., Gares, P. A., & Colby, J. D. (2002). Techniques for GIS modeling of coastal dunes. *Geomorphology*, *48*(1–3), 289–308. [https://doi.org/10.1016/S0169-555X\(02\)00186-1](https://doi.org/10.1016/S0169-555X(02)00186-1)
- Burvingt, O., Masselink, G., Russell, P., & Scott, T. (2017). Classification of beach response to extreme storms. *Geomorphology*, *295*(C), 722–737. <https://doi.org/10.1016/j.geomorph.2017.07.022>
- Emanuel, K. A. (2013). Downscaling CMIP5 climate models shows increased tropical cyclone activity over the 21st century. *Proceedings of the National Academy of Sciences*, *110*(30), 12219–12224. <https://doi.org/10.1073/pnas.1301293110>
- Farris, G. S., Smith, G. J., Crane, M. P., Demas, C. R., Robbins, L. L., & Lavoie, D. L. (2007). Science and the storms. *U. S. Geological Survey Circular*.
- Fernández-Montblanc, T., Duo, E., & Ciavola, P. (2020). Dune reconstruction and revegetation as a potential measure to decrease coastal erosion and flooding under extreme storm conditions. *Ocean & Coastal Management*, *188*, 105075. <https://doi.org/10.1016/j.ocecoaman.2019.105075>
- Fletcher, C. S., Rambaldi, A. N., Lipkin, F., & McAllister, R. R. J. (2016). Economic, equitable, and affordable adaptations to protect coastal settlements against storm surge inundation. *Regional Environmental Change*, *16*(4), 1023–1034. <https://doi.org/10.1007/s10113-015-0814-1>
- George Bevan, Matthew J. Lato, & Michael Fergusson. (2012). Gigapixel Imaging and Photogrammetry: Development of a New Long Range Remote Imaging Technique. *Remote Sensing*, *4*(10), 3006–3021. <https://doi.org/10.3390/rs4103006>
- Gesch, D. (2007). Topography-based analysis of Hurricane Katrina inundation of New Orleans. *US Geological Survey Circular*, *1306*, 53–56.

- Hartigan, J. A., & Wong, M. A. (1979). Algorithm AS 136: A K-Means Clustering Algorithm. *Journal of the Royal Statistical Society. Series C (Applied Statistics)*, 28(1), 100–108. JSTOR.  
<https://doi.org/10.2307/2346830>
- Houser, C., Wernette, P., Rentschlar, E., Jones, H., Hammond, B., & Trimble, S. (2015). Post-storm beach and dune recovery: Implications for barrier island resilience. *Geomorphology*, 234(C), 54–63. <https://doi.org/10.1016/j.geomorph.2014.12.044>
- Jackson, D. W. T., Cooper, J. A. G., & del Rio, L. (2005). Geological control of beach morphodynamic state. *Marine Geology*, 216(4), 297–314. <https://doi.org/10.1016/j.margeo.2005.02.021>
- Lee, K., & Park, J. (2019). Comparison of UAV Image and UAV LiDAR for Construction of 3D Geospatial Information. *Sensors and Materials*, 31(10(3)), 3327–3334.  
<https://doi.org/10.18494/SAM.2019.2466>
- Liu, Z., Wang, H., Zhang, Y. J., Magnusson, L., Loftis, J. D., & Forrest, D. (2020). Cross-scale modeling of storm surge, tide, and inundation in Mid-Atlantic Bight and New York City during Hurricane Sandy, 2012. *Estuarine, Coastal and Shelf Science*, 233, 106544.  
<https://doi.org/10.1016/j.ecss.2019.106544>
- Masselink, G., Scott, T., Poate, T., Russell, P., Davidson, M., & Conley, D. (2016). The extreme 2013/2014 winter storms: Hydrodynamic forcing and coastal response along the southwest coast of England. *Earth Surface Processes and Landforms*, 41(3), 378–391.  
<https://doi.org/10.1002/esp.3836>
- Penning-Rowsell, E., & Pardoe, J. (2015). The distributional consequences of future flood risk management in England and Wales. *Environment and Planning C: Government and Policy*, 33(5), 1301–1321. <https://doi.org/10.1068/c13241>
- Pye, K., & Blott, S. J. (2016). Assessment of beach and dune erosion and accretion using LiDAR: Impact of the stormy 2013–14 winter and longer term trends on the Sefton Coast, UK. *Geomorphology*, 266, 146–167. <https://doi.org/10.1016/j.geomorph.2016.05.011>

- R Core Team. (2013). *R: A Language and Environment for Statistical Computing*. R Foundation for Statistical Computing. <http://www.R-project.org/>
- Richter, A., Faust, D., & Maas, H.-G. (2013). Dune cliff erosion and beach width change at the northern and southern spits of Sylt detected with multi-temporal Lidar. *Catena*, *103*, 103–111. <https://doi.org/10.1016/j.catena.2011.02.007>
- Roebeling, P., d'Elia, E., Coelho, C., & Alves, T. (2018). Efficiency in the design of coastal erosion adaptation strategies: An environmental-economic modelling approach. *Ocean & Coastal Management*, *160*, 175–184. <https://doi.org/10.1016/j.ocecoaman.2017.10.027>
- Sallenger, A., Wright, W., Lillycrop, J., Howd, P., Stockdon, H., Guy, K., & Morgan, K. (2007). Extreme changes to barrier islands along the central Gulf of Mexico coast during Hurricane Katrina. In *U. S. Geological Survey Circular* (pp. 114–119). USGeological Survey.
- Saye, S. E., van Der Wal, D., Pye, K., & Blott, S. J. (2005). Beach–dune morphological relationships and erosion/accretion: An investigation at five sites in England and Wales using LIDAR data. *Geomorphology*, *72*(1), 128–155. <https://doi.org/10.1016/j.geomorph.2005.05.007>
- Sekovski, I., Stecchi, F., Mancini, F., & Rio, L. D. (2014). Image classification methods applied to shoreline extraction on very high-resolution multispectral imagery. *International Journal of Remote Sensing*, *35*(10), 3556–3578. <https://doi.org/10.1080/01431161.2014.907939>
- Sellick, J. (2006). *Towards a future maritime policy for the union: A European vision for the oceans and seas*. *17*, 33–35.
- SNAP - ESA Sentinel Application (Version 7.0.3). (2019). [Computer software]. <http://step.esa.int>
- Stoker, J., Tyler, D., Turnipseed, D., Van Wilson, K., & Oimoen, M. (2009). Integrating Disparate Lidar Datasets for a Regional Storm Tide Inundation Analysis of Hurricane Katrina. *Journal of Coastal Research*, *25*(6), 66–72. <https://doi.org/10.2112/SI53-008.1>
- Sullivan, K., & Uccellini, L. (2013). Hurricane/Post-Tropical Cyclone Sandy, October 22–29, 2012. *Miami: Department of Commerce National Oceanic and Atmospheric Administration*.

Woolard, J. W., & Colby, J. D. (2002). Spatial characterization, resolution, and volumetric change of coastal dunes using airborne LIDAR: Cape Hatteras, North Carolina. *Geomorphology*, *48*(1–3), 269–287. [https://doi.org/10.1016/S0169-555X\(02\)00185-X](https://doi.org/10.1016/S0169-555X(02)00185-X)

Yang, X. (2008). *Remote Sensing and Geospatial Technologies for Coastal Ecosystem Assessment and Management*. Springer Science & Business Media.

## 7 APPENDIX A

---

### 7.1 R CODE FOR CREATION OF DSMs FROM RAW LIDAR DATA

```
# CONSTANTS
PRE_FOLDER <- "F:/ARS/Shoreline_Change/PRE"
POST_FOLDER <- "F:/ARS/Shoreline_Change/POST"
RESULTS_FOLDER <- "F:/ARS/Shoreline_Change"

# Setup packages and Libraries
install.packages("lidR")
library(lidR)
install.packages("mapview")
library(mapview)

#####
# PRE HURRICANE SECTION
# Setwd
wd<-setwd(PRE_FOLDER)

#Read in catalog
ctg_nj_pre<-readLAScatalog(wd)
summary(ctg_nj_pre)
plot(ctg_nj_pre)

# add map background. EPSG3615.
crs_nj<-sp::CRS("+init=epsg:3615")
projection(ctg_nj_pre)<-crs_nj
plot(ctg_nj_pre, map=TRUE)

# Attempt to calculate full PRE raster
wd<-setwd(PRE_FOLDER)
ctg_nj_pre<-readLAScatalog(wd)
dsm_full_pre = grid_canopy(ctg_nj_pre, res=2, algorithm = dsmtin())
setwd(RESULTS_FOLDER)
writeRaster(dsm_full_pre, filename = "DSM_FULL_PRE.tif", format = "GTiff", ove
rwrite = TRUE)

#####
# POST HURRICANE SECTION
wd<- setwd(POST_FOLDER)

# Read in the las catalog
ctg_nj_post<-readLAScatalog(wd)
summary(ctg_nj_post)
```

```

plot(ctg_nj_post)

# add map background. EPSG3615.
crs_nj<-sp::CRS("+init=epsg:3615")
projection(ctg_nj_post)<-crs_nj
plot(ctg_nj_post, map=TRUE)

# Attempt to calculate full POST raster
wd<- setwd(POST_FOLDER)
ctg_nj_post<-readLAScatalog(wd)
dsm_full_post = grid_canopy(ctg_nj_post, res=2, algorithm = dsmtin())
setwd(RESULTS_FOLDER)
writeRaster(dsm_full_post, filename = "DSM_FULL_POST.tif", format = "GTiff", o
verwrite = TRUE)

```

## 7.2 R CODE FOR CREATION OF DAMAGE RASTER

```

#####
# RASTER MATH SECTION
# Calculate difference raster
post_pre<-dsm_full_post-dsm_full_pre
plot(post_pre)
setwd(RESULTS_FOLDER)
writeRaster(post_pre, filename = "Damage_FULL.tif", format = "GTiff", overwrit
e = TRUE)

```

## 7.3 R CODE FOR UNSUPERVISED IMAGERY CLASSIFICATION AND MODAL FILTERING

```

# Import libraries (already installed)
library(RStoolbox)
library(raster)

# Southern Image - stack bands into a single raster
wd<-setwd("C:/ARS/Shoreline_Change/Sentinel/T18SWJ_BANDS")
Sb2 <- brick('b2.img')
Sb3 <- brick('b3.img')
Sb4 <- brick('b4.img')
Sb5 <- brick('b5.img')
Sb6 <- brick('b6.img')

```

```

Sb7 <- brick('b7.img')
Sb8 <- brick('b8.img')
Sb8A <- brick('b8A.img')
Sb11 <- brick('b11.img')
Sb12 <- brick('b12.img')

south <-stack(Sb2,Sb3,Sb4,Sb5,Sb6,Sb7,Sb8,Sb8A,Sb11,Sb12)
plotRGB(south, r = 3, g = 2, b = 1, stretch = "lin")
writeRaster(south, filename="south.tif", options="INTERLEAVE=BAND", overwrite=
TRUE)

# northern Image - stack bands into a single raster
wd<-setwd("C:/ARS/Shoreline_Change/Sentinel/T18TWK_BANDS")
Nb2 <- brick('b2.img')
Nb3 <- brick('b3.img')
Nb4 <- brick('b4.img')
Nb5 <- brick('b5.img')
Nb6 <- brick('b6.img')
Nb7 <- brick('b7.img')
Nb8 <- brick('b8.img')
Nb8A <- brick('b8A.img')
Nb11 <- brick('b11.img')
Nb12 <- brick('b12.img')

north <-stack(Nb2,Nb3,Nb4,Nb5,Nb6,Nb7,Nb8,Nb8A,Nb11,Nb12)
plotRGB(north, r = 3, g = 2, b = 1, stretch = "lin")
writeRaster(north, filename="north.tif", options="INTERLEAVE=BAND", overwrite=
TRUE)

# Coregister the Imagery
wd<-setwd("C:/ARS/Shoreline_change/Sentinel")
north_south<- RStoolbox::coregisterImages(north, south, verbose = TRUE)
# "Identified shift in map units (x/y): 0/0"

# Histogram Match and Merge
# north + south
north_hm<-histMatch(north, south)
north_south<-merge(north_hm, south)
plotRGB(north_south, r = 3, g = 2, b = 1, stretch = "lin", axes= TRUE, main="n
orth, south merged")

# Output our merged image
writeRaster(north_south, filename="NJ_S2_merged.tif", options="INTERLEAVE=BAND
", overwrite=TRUE)

# Unsupervised Classification
# read in raster from file again to allow this part of the code to be run afte
r closing session:

```

```
wd<-setwd("C:/ARS/Shoreline_change/Sentinel")
north_south <- brick("NJ_S2_merged.tif")

set.seed(100)
uc3<-unsuperClass(north_south, nClasses=3, nStarts = 50, nSamples = 1000)
plot(uc3$map)
writeRaster(uc3$map, filename="NJ_uc_3class.tif", options="INTERLEAVE=BAND", o
verwrite=TRUE)

# Modal Filtering
window <-matrix(1,7,7)
NJ_uc3_mode<-focal(uc3$map, w=window, fun = modal)
NJ_uc3_mode$layer
writeRaster(NJ_uc3_mode$map, filename="NJ_uc3_mode.tif", options="INTERLEAVE=B
AND", overwrite=TRUE)
```

## APPENDIX B

---

### 1:20,000 MAP SERIES OF MORPHOLOGICAL CHANGE

Please note, this page has intentionally been left blank, the map series will begin on the following page.